ISIJ International, Vol. 55 (2015), No. 4, pp. 894–903

Development of Continuous Steelmaking Slag Solidification Process Suitable for Sensible Heat Recovery

Hiroyuki TOBO,[1)]* Yasutaka TA,[1)] Michihiro KUWAYAMA,[2)] Yuki HAGIO,[3)] Kazuya YABUTA,[4)] Hirokazu TOZAWA,[5)] Toshihiro TANAKA,[6)] Kazuki MORITA,[7)] Hiroyuki MATSUURA[8)] and Fumitaka TSUKIHASHI[8)]

1) Steel Research Laboratory, JFE Steel Corporation, 1, Kawasaki-cho, Chuo-ku, Chiba, 260-0835 Japan. 2) Formerly Steel Research Laboratory, JFE Steel Corporation. Now at Shinagawa Refractories Co., Ltd, 1, Mizushimakawasakidori, Kurashiki, 712-0874 Japan. 3) East Japan Works, JFE Steel Corporation, 1, Kawasaki-cho, Chuo-ku, Chiba, 260-0835 Japan. 4) Slag Business Planning & Control Dept., JFE Steel Corporation, 2-2-3, Uchisaiwaicho, Chiyoda-ku, Tokyo 100-0011 Japan. 5) Formerly Technology Planning Dept., JFE Steel Corporation. Now at The Iron and Steel Institute of Japan, 3-2-10, Nihonbashi-Kayabacho, Chuo-ku, Tokyo, 103-0025 Japan. 6) Division of Materials and Manufacturing Science, Graduate School of Engineering Osaka University, 1-1, Yamadaoka, Suita, Osaka, 565-0871 Japan. 7) Department of Materials Engineering, Graduate School of Engineering, The University of Tokyo, 7-3-1, Hongo, Bunkyo-ku, Tokyo, 113-8656 Japan. 8) Department of Advanced Materials Science, Graduate School of Frontier Sciences, The University of Tokyo, 5-1-5, Kashiwanoha, Kashiwa, Chiba, 277-8561 Japan.

(*Received on September 12, 2014; accepted on December 10, 2014; originally published in Tetsu-to-Hagané, Vol. 99, 2013, No. 12, pp. 683–692*)

The COURSE50 project aims at developing technologies to reduce CO_2 emissions from steel works by approximately 30% in Japan. In order to supply the energy required to separate CO_2, a technology for recovering sensible heat from steelmaking slag is being developed as one theme of COURSE50. A twin roll type continuous slag solidification process to obtain a shape suitable for sensible heat recovery was investigated.

Sheet-like slag was shaped to a thickness of about 7 mm in a twin roll pilot-scale experiment. The slag thickness depended on the adhesion of the molten slag rather than the thickness of the solidified slag on the roll. The slag condition suitable for the twin roll method was identified as a liquid phase ratio of 60% or more. Based on a laboratory-scale experiment and heat transfer calculations, a combination process using the twin roll method and a countercurrent flow packed bed is expected to achieve a heat recovery ratio of 30% or more from sheet-like slag.

KEY WORDS: steelmaking slag; solidification; heat recovery; sensible heat; thickness.

1. Introduction

To address the issue of global warming, Japan's steelmakers are engaged in a National Project called "Environmentally Harmonized Steelmaking Process Technology Development (COURSE50)" (COURSE50: CO_2 Ultimate Reduction in Steelmaking Process by Innovative Technology for Cool Earth 50)" to develop a technology that dramatically reduces CO_2,[1,2)] with the aim of reducing CO_2 emissions from steel works by approximately 30%. Two technologies for reduction of CO_2 emissions are under development: 1) Use of hydrogen to reduce iron ore in the blast furnace,[3)] and 2) Separation and recovery of generated CO_2.[4,5)]

Two approaches to separation and recovery of CO_2 are under study, namely, chemical absorption and physical adsorption. With the chemical absorption technology, thermal energy is required to regenerate CO_2-laden chemical absorbents by separating CO_2 from the absorbents.[6)] In COURSE50, a technology that effectively uses unused sensible heat and waste heat in the steel works as sources of this thermal energy is being developed. One of the themes in this project is development of a process for recovering sensible heat from steelmaking slag, which has the highest temperature and represents the largest amount of unused waste heat in the steel works.

The worldwide energy potential of slag has been estimated at 370×10^3 TJ/y.[7)] Various processes have been developed for recovery of sensible heat from slag. In sensible heat recovery from blast furnace slag, the air granulation method,[8,9)] rotating drum granulation method,[10)] and stirring granulation method[11)] were examined with practical scale equipment. Recently, the rotary cup atomizer method[12,14)] and fluidized bed direct charging method[15)] have also been examined.

The only example of practical application of an air granulation system for converter slag was at NKK Corp.'s Fukuyama Works (now JFE Steel West Japan Works (Fukuyama District)), which was used in sensible heat recovery of steelmaking slag.[15,16)] However, because the product air-granulated slag consists of small, spherical particles, its uses were limited. The air granulation system was later abolished, as various other types of low cost exhaust

* Corresponding author: E-mail: h-tobo@jfe-steel.co.jp
DOI: http://dx.doi.org/10.2355/isijinternational.55.894

heat recovery equipment such as CDQ (coke dry quenching) were constructed subsequently.

In this study, we propose combining a twin roll method for slag solidification and a packed bed method for heat exchange from slag to air in order to realize efficient recovery of the sensible heat of slag, which has low thermal conductivity. The twin roll method is a process in which two rolls are placed in contact and rotated upward. Molten slag is supplied between the rolls, where it is cooled and solidified in sheet-like shape on the roll surfaces. Although practical application of the twin roll slag solidification process has not been achieved with blast furnace slag,[17,18] the process has been used practically as a cooling solidification technology for the molten slag residue of municipal waste incineration.[19,20] Although this twin roll method has a record of use with low basicity slags such as the blast furnace slag and municipal waste molten slag, it has not been applied to high basicity steelmaking slag.

In this study, the conditions for slag forming with water-cooled rolls were investigated in order to develop a continuous steelmaking slag solidification process suitable for sensible heat recovery.

2. Experimental Method

2.1. Experimental Method for Forming Sheet-like Slag with Single Roll Apparatus

To confirm whether steelmaking slag can be formed to a sheet shape with a roll, an experimental apparatus employing a single roll method was produced. A schematic diagram of the experimental apparatus is shown in **Fig. 1**, and its specification is shown in **Table 1**. This apparatus consists of a cooling roll, shape control roll, conveyor, and sensible heat recovery equipment mounted on a platform truck. The cooling roll and shape control roll were equipped internal water cooling. The water flow rate was 80 L/min. **Figure 2**(a) shows the method of controlling the slag solidification thickness. The solidification thickness is adjusted by the rotational speed of the cooling roll. The shape control roll was provided to expand the slag to the width of the roll. The gap between the shape control roll and the cooling roll was set to be 5 mm. In the following, the experiment with this apparatus will be called the single roll laboratory experiment.

The experimental method was as follows. First, 30–40 kg of steelmaking slag was melted at 1 873 K in a plasma melting furnace. The molten slag temperature was measured with expendable thermocouples. Next, the truck was moved to the position where it touched the plasma furnace, and the roll and conveyor were rotated. The molten slag was then supplied to the cooling roll from the plasma furnace via a chute. The molten slag flow was controlled to constant rate by controlling the tilting inclination of the plasma furnace. The slag was solidified on the surface of the rotating roll. The solidified sheet-like slag fell on the conveyor after a half-turn on the roll, and was carried by the conveyer and dropped from the end of conveyor into the sensible heat recovery equipment shown in Fig. 2(b). The temperatures of the slag on the chute and the roll surface and at the end of the conveyor were measured by two infrared thermography devices.

Two kinds of slag were used in this experiment. Slag A was a high basicity decarburization slag generated by the converter. Slag B was a low basicity chromium ore smelting reduction slag. The chemical compositions of the slag are shown in **Table 2**.

The lid of the heat recovery equipment was closed after filling the vessel with solidified slag. Air for heat exchange was passed through the heat recovery at 200 L/min from the

Table 1. Specification of single roll type slag solidification and heat recovery apparatus.

Equipment		Specifications
Cooling roll	Dimensions	Φ0.35 m×W0.5 m
	Material	SS400
	Rotation speed	3.4–20.5 rpm
	Cooling water flow rate	80 L/min
Shape control roll	Dimensions	Φ0.16 m×W0.5 m
	Material	SS400
	Rotation speed	7.7–46.9 rpm
Conveyer	Dimensions	W0.37 m×L2.0 m
	Material	SUS304
	Speed	5.2–31.4 m/min
Heat recovery apparatus	Dimensions (inner)	Φ0.3 m×D0.65 m
	Air flow rate	20–200 L/min
Plasma furnace	Heating method	Nontransfer type plasma
	Torch electric power	100 kW×2
	Plasma gas	Ar
	Gas flow rate	100–160 L/min×2
	Furnace dimensions (inner)	Φ0.4 m×D0.35 m

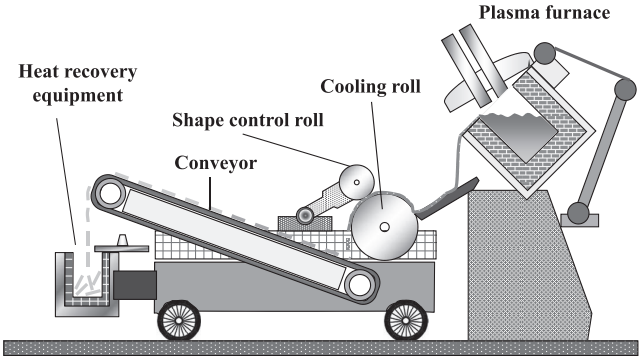

Fig. 1. Schematic diagram of single roll type slag solidification and heat recovery apparatus.

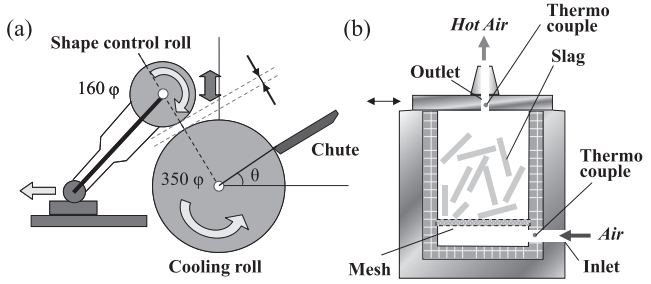

Fig. 2. (a) slag thickness control method and (b) heat recovery equipment.

Table 2. Chemical composition of steelmaking slag.

Slag	CaO	SiO_2	Al_2O_3	MgO	MnO	P_2O_5	T.Fe	M.Fe	FeO	S	F.CaO	CaO/SiO_2
A	42.4	11.1	1.8	6.1	3.5	2.2	22.5	2.1	13.2	0.03	6.1	3.8
B	34.2	15.7	17.1	15.6	0.3	0.03	4.1	1.1	3.3	0.55	0.9	2.2

equipment bottom. The air temperatures at the inlet and exit of the equipment and the temperature of the shell were measured at intervals of 1 s with K type sheathed thermocouples.

2.2. Experimental Method for Forming Sheet-like Slag with Twin Roll Apparatus

With the single roll laboratory apparatus, leakage of molten slag from the space between the roll and chute was a problem. Therefore, a twin roll method was adopted in a pilot experimental plant of practical scale. A method in which two rolls are rotated in the inward direction to form sheet-like slag was also developed in recent years.[21,22] However, in order to secure a longer slag solidification time, the same method as that of the equipment developed and commercialized by Akashi[20] was adopted. In this particular method, the two rolls are placed in contact and are each rotated in an outward direction. Therefore, the slag is drawn upward with the rolls. A schematic diagram of the pilot plant is shown in **Fig. 3**. The equipment specification is shown in **Table 3**. The plant comprises two cooling rolls which continuously solidify the slag, a slag ladle tilting machine for supplying molten slag to the rolls at a constant flow rate, and a conveyer for transporting the slag which has been formed by the rolls. In order to enhance cooling of the slag, the cooling rolls are made of copper material and are equipped with internal water cooling. Assuming a supply rate of 1 t/min for the molten slag and a thickness of about 5 mm for the slag when solidified, we designed large-scale rolls with an outer diameter of 1.6 m and roll width of 1.5 m. The ladle tilting device can accommodate the slag ladles which are used to transport molten slag in the steelmaking shop, and can tilt a ladle at a constant speed by means of a hydraulic cylinder. The conveyor transporting the high temperature solidified slag after roll-forming is made of stainless steel, and its back side is equipped with spray nozzles for cooling. The slag used in this experiment was the slag obtained from the above-mentioned chromium ore smelting reduction furnace. In the following, the experiment with this plant will be called the twin roll pilot experiment.

An experiment was performed with the twin roll type steelmaking slag solidification pilot plant by the following procedure. The tilting device was pushed up at a constant speed by the hydraulic cylinder, and molten slag was fed from the slag ladle into the gap between the two rolls via a chute. The two rolls were rotated in an outward direction, and the slag which was cooled and solidified on the roll surface adhered to the rolls and was drawn upward as the rolls rotated. After rotating approximately 180°, the slag dropped onto the conveyor. The solidified slag was transported by the conveyor and dropped from the end of the conveyor into a pit. In the pit, the slag was either cooled by water-sprinkling or allowed to cool by natural radiation, and was then removed with a shovel. The temperature of the molten

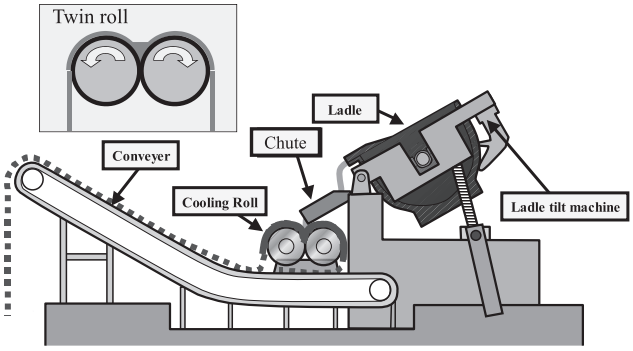

Fig. 3. Schematic diagram of twin roll type continuous slag solidification pilot plant.

Table 3. Specification of twin roll type continuous slag solidification pilot plant.

Equipment	Specifications	
Cooling roll	Dimensions	Φ1.6 m×W1.5 m
	Number of rolls	2
	Material	Cu
	Rotation speed	Max.20 rpm
	Cooling water flow rate	125–130 m^3/h/roll
Ladle tilt machine	Tilt speed	Max.6.5°/min
	Load	Max.140 t
Conveyer	Dimensions	W1.3 m×L14.5 m
	Lifting height	5.5 m
	Speed	Max.25 m/min
	Material	SUS304

slag discharged from the ladle was measured with a radiation thermometer. The temperatures of the slag on the rolls and on the conveyor were measured by infrared thermography. In both cases, emissivity was assumed to be 0.92.

2.3. Thermal Conductivity, Specific Heat, and Viscosity Measurement Methods

Thermal conductivity, specific heat, and viscosity, which are important values for heat recovery and roll solidification of slag, were measured.

The thermal conductivity of the slag was measured by the hot wire method.[23] First, about 200 g of slag was placed in a zirconia crucible with an inner diameter of 43 mm, and was melted at 1 773 K. The thermal conductivity of the slag was then measured each at intervals of 50 K until the temperature reached 573 K.

The specific heat of the slag was measured with a fall type calorimeter. Here, 12 g of slag was placed in a platinum crucible, and the temperature was increased to 962–1 825 K and maintained for 1 hour. After holding at this temperature, the crucible was unloaded into the fall type calorimeter

under the furnace, the rise in water temperature was measured, and the specific heat was calculated.

The viscosity of the slag was measured with a high temperature rotary viscometer. A graphite crucible with an inner diameter of 40 mm and a graphite rotor with an outer diameter of 30 mm were used for the molten slag.

230 g of slag was heated to 1 823 K in a crucible with argon. The viscosity of the slag was measured by rotating the rotor into the molten slag, and was then measured each at intervals of 50 K until 1 673 K.

3. Experimental Results

3.1. Results of Single Roll Laboratory Experiment

In the single roll laboratory experiment, the molten slag extended to 1/2 or more of the width on the roll surface, and was formed to the desired sheet-like shape. Not only solidified slag but also slag in a semi-molten state was observed on the roll. When the solidified slag fell from the end of conveyor, it broke up into pieces about 20–80 mm in size. **Figure 4** shows the typical appearances of the solidified sheet-like slag A and slag B after break-up at the end of the conveyor. The sheet-like slag had a rough surface, and also included pieces with curved shapes.

Figure 5 shows the relationship between the slag thickness and cooling roll rotation speed for slag A. The frequency of each thickness of the sheet-like slag at rotation speeds of 5, 7, and 10 rpm is shown in Fig. 5(b). The slag solidification thickness and scattering of the thickness values decrease with increasing roll rotation speed. The predominant thickness of slag A is 1–2 mm at all rotational speeds. Thicknesses over 5 mm, which is the same as the gap between the cooling roll and the shape control roll, were observed at 5 rpm. Regarding the slag with a thickness of 5 mm or more, this slag failed to solidify continuously on the roll and broke off once. After a certain time, it was picked up again by the roll, and then lifted the shape control roll while passing between the rolls.

Figure 6 shows relationship between the slag thickness and cooling roll rotation speed for slag B. In comparison with slag A, in the case of slag B, the fluidity of the molten slag tended to be low, the solidified thickness was thick, and the pieces were large.

Figure 7 shows effect of the molten slag supply position on the slag thickness of slag B. When the trough position was 60°, the molten slag passed over the roll while still in the molten state. However, when the chute position was lowered to 35°, the molten slag adhered on the roll and solidified. The thickness also became smaller, and the thickness of 2–3 mm accounted for the largest percentage, as shown in Fig. 7(b).

Figure 8 shows the slag surface temperature at the end of the conveyor. In this figure, the x-axis indicates time from the point where supply of molten slag to the rolls began. As there was no difference in the temperature at the rotation speeds of 5 rpm and 10 rpm, it can be understood that a temperature of approximately 1 300 K or more was secured before heat recovery.

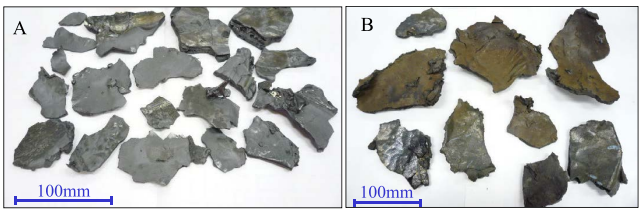

Fig. 4. Appearance of sheet-like slag obtained in laboratory scale experiment. (Online version in color.)

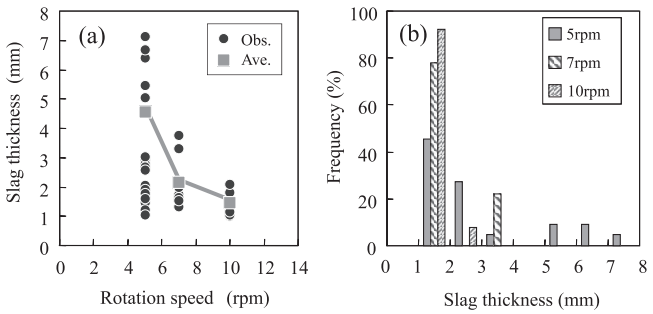

Fig. 5. Relationship between cooling roll rotation speed and thickness of slag A ((a) thickness, (b) frequency).

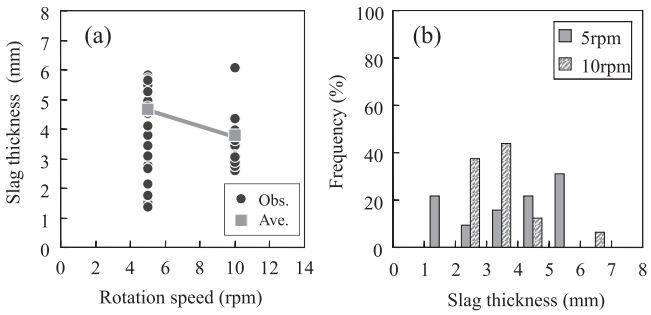

Fig. 6. Relationship between cooling roll rotation speed and thickness of slag B ((a) thickness, (b) frequency).

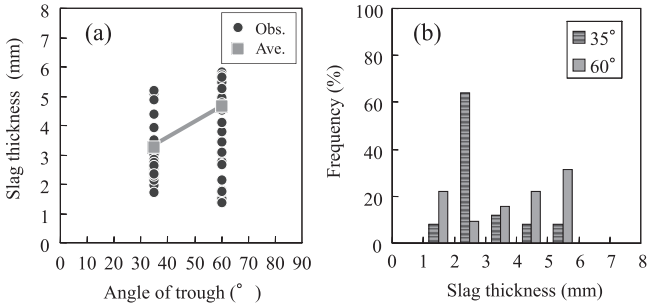

Fig. 7. Effect of molten slag supply position on thickness of slag B ((a) thickness, (b) frequency).

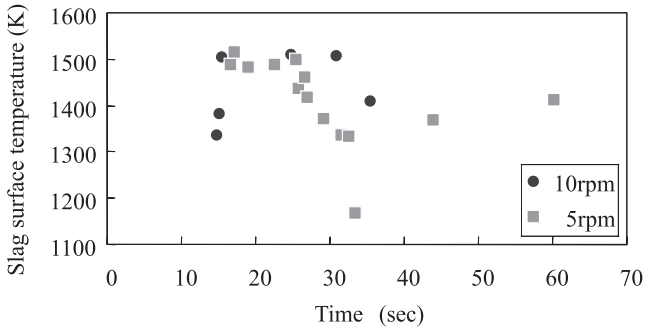

Fig. 8. Slag surface temperature at end of conveyer.

3.2. Results of Sensible Heat Recovery Experiment

Figure 9 shows an example of the heat recovery experiment results. In this experiment, 6.55 kg of slag was charged to the heat recovery equipment, and the average bed thickness was 69 mm. Because the slag was sheet-shaped, the filling fraction was only 0.41. Figure 9 shows the air temperatures at the inlet and the outlet, together with the heat recovery ratio. The maximum temperature of the air at the outlet was 860 K. The heat recovery ratio was calculated from the difference between the outlet air temperature and 413 K, assuming the thermal capacity of slag at 1 823 K is 100%. Considering application to CO_2 separation and recovery, the air temperature range of 413 K or more is effective for CO_2 separation from the chemical absorption liquid. The heat recovery ratio was 31.2% in this case.

3.3. Results of Twin Roll Pilot Experiment

Figure 10 shows a typical view of the twin roll pilot experiment. When the molten slag had sufficient fluidity, it spread across the full width of the rolls and was continuously solidified by the rolls. In the initial period of the pilot experiments, because the fluidity of the molten slag was low, it did not flow from the ladle, or it solidified between the rolls. After the fluidity of the molten slag was improved by increasing the Al_2O_3 content, it was possible to form the slag continuously to a sheet-shape with the twin roll apparatus. **Figure 11** shows the effects of the Al_2O_3 content and slag temperature on the formability of the slag in the pilot experiments. In this figure, the symbol ○ indicates that continuous forming on the whole width of the rolls was possible, △ indicates continuous forming over 1/2–1/3 of the roll width, and × indicates that forming was not possible. A combination of a high Al_2O_3 content and high temperature was necessary for continuous forming of the sheet-shape slag on the whole width of the rolls.

Figure 11 shows the lines of the liquid phase ratios 40%, 60%, and 80%, which were calculated by the thermodynamic calculation program FactSage 6.3. The database used was FT oxid. Because the FeO content was low, the calculation was made for four elements (CaO, SiO_2, Al_2O_3, and MgO), and it was assumed that CaO/SiO_2=2.2 and the MgO content is constant at 20%. A liquid phase ratio of 60% or more is necessary in order to ensure that the molten slag extends over the whole width of the rolls.

The solidified slag after cooling is shown in **Fig. 12**. The slag broke up into smaller pieces as it dropped from the end of the conveyor and into the pit, where it was crushed. From observation of the recovered slag, it was noted that the surface of the slag that had been in contact with the roll was flat and hard, and its free surface was porous and rough.

The influence of the cooling roll rotation speed on slag thickness is shown in **Fig. 13**. The cooling roll rotation speed for obtaining the thickness of 5 mm was estimated from the single roll laboratory experiment. However, the average solidification thickness was approximately 10 mm at 5 rpm in the twin roll pilot experiment. In other words, the thickness of the slag formed in the twin roll pilot experiment was about twice that in the single roll laboratory experiment.

To reduce the solidification thickness of the slag, the roll

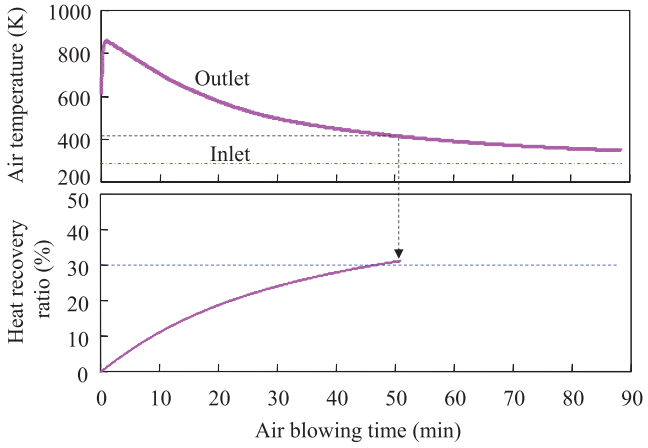

Fig. 9. Heat recovery result in laboratory scale experiment.

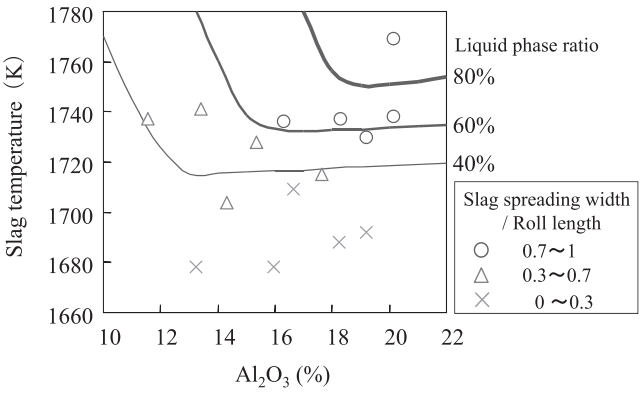

Fig. 11. Effect of Al_2O_3 content and slag temperature on formability of slag in pilot experiment.

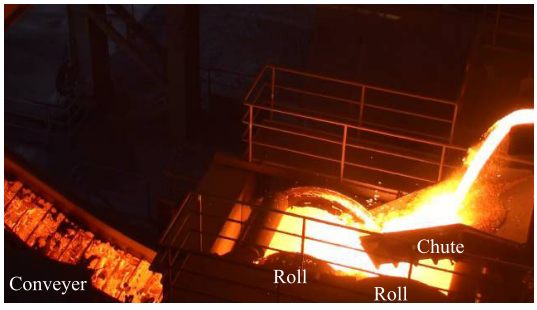

Fig. 10. View of pilot experiment by twin roll type continuous slag solidification process. (Online version in color.)

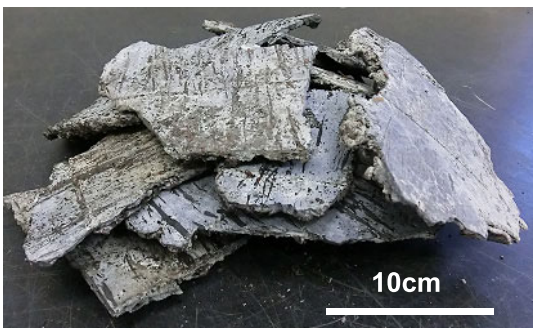

Fig. 12. Appearance of solidified slag after twin roll process. (Online version in color.)

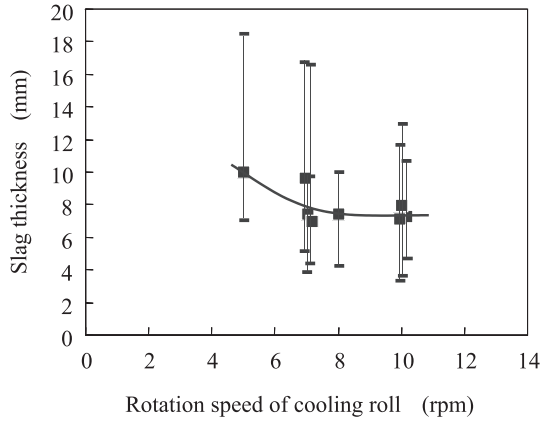

Fig. 13. Relationship between cooling roll rotation speed and slag thickness in pilot experiment.

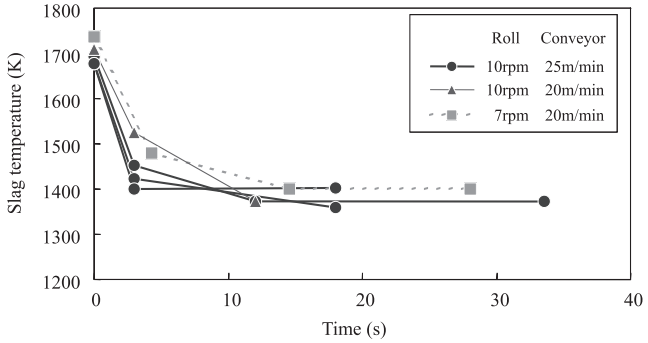

Fig. 14. Change of slag surface temperature in twin roll process with different transfer rates.

rotation speed was increased to 10 rpm. In the rotation speed range of 8–10 rpm, the average thickness decreased to 7–8 mm. **Figure 14** shows an example of the results of slag surface temperature measurements by infrared thermography. The slag surface temperature decreases by 200–250 K when the slag solidifies on the rolls. The temperature drop on the conveyor was slight, and the slag temperatures at the conveyor end were about 1 373 K.

Slag B, which contains neither phosphorus nor boron, disintegrates after treatment by slow cooling.[24] In contrast, after the roll forming, slag B retains the sheet shape. Powder X-ray diffraction was performed to investigate the change in mineral phases. **Figure 15** shows the X-ray diffraction patterns of slowly-cooled slag (a) and sheet-shaped slag after roll forming (b). The mineral phases were dicalcium silicate ($2CaO{\cdot}SiO_2$), gehlenite ($2CaO{\cdot}Al_2O_3{\cdot}SiO_2$), akermanite ($2CaO{\cdot}MgO{\cdot}2SiO_2$), periclase (MgO), and spinel ($MgO{\cdot}Al_2O_3$). γ-$2CaO{\cdot}SiO_2$ exists in the slowly-cooled slag but does not exist in the sheet-shaped slag after roll forming. In phase transformation of the γ type in the cooling process, the density of dicalcium silicate changes, causing this phase to disintegrate. Because slag (b) was quenched from molten slag by the water-cooled rolls, the dicalcium silicate was a β type without transforming to the γ type. Therefore, it did not disintegrate and maintained the sheet shape.

3.4. Results of Measurement Slag Thermal Conductivity, Enthalpy, and Viscosity

The thermal conductivity of slag B, which was the chromium ore smelting reduction furnace slag, could not be measured because it contained carbon, which reacted with the platinum wire. It was possible to measure the thermal conductivity of the decarburization slag. The results of measurement of the thermal conductivity of decarburization slag with basicity CaO/SiO_2=3.3 are shown in **Fig. 16**. Thermal conductivity showed its maximum value at 1 500 K, and decreased at both higher and lower temperatures. However, in most temperature ranges, thermal conductivity showed a small value of 0.5 W/(m·K) or less.

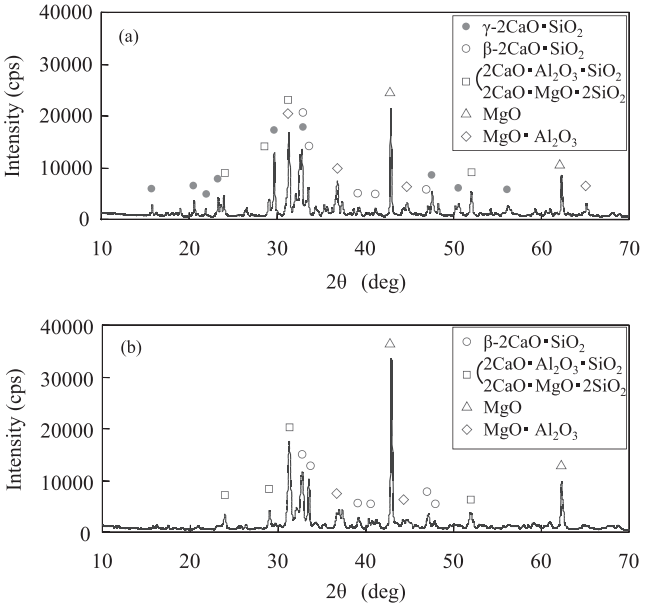

Fig. 15. X-ray diffraction pattern of solidified slag. (a) Slow cooled slag, (b) Sheet-like slag made by twin roll process.

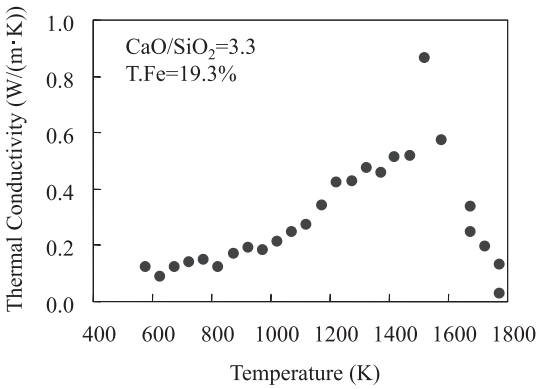

Fig. 16. Effect of temperature on thermal conductivity of steelmaking slag.

The relation between the enthalpy of slag B and temperature is shown in **Fig. 17**. Enthalpy is based at 293 K and increases linearly from 969 K to 1 574 K and from 1 723 K to 1 825 K. The slopes of these straight lines were the average enthalpy Cp in these temperature ranges. The results were Cp=1.01 J/(g·K) from 969 K to 1 574 K, 1 825 K Cp=0.503 J/(g·K) from 1 723 to 1 825 K.

The effect of temperature on the viscosity of slag B is shown in **Fig. 18**. Viscosity was 1.61 Pa·s at 1 673 K. Because viscosity was too high at 1 650 K or less, measurement was not possible with the high temperature rotational viscometer.

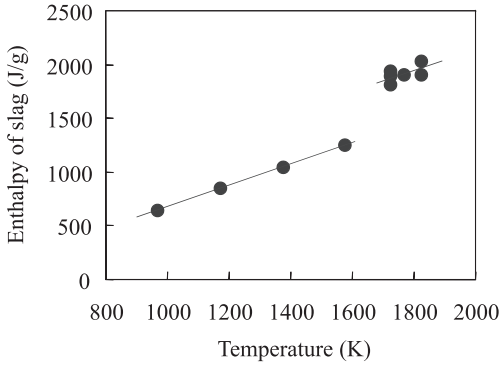

Fig. 17. Relationship between enthalpy of slag B and temperature.

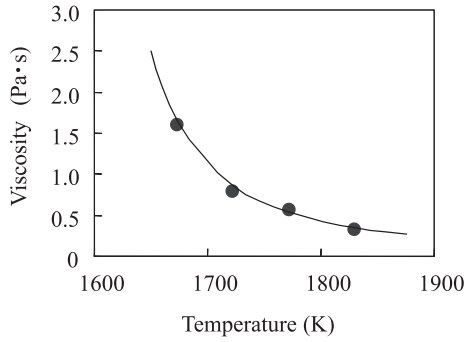

Fig. 18. Effect of temperature on viscosity of slag B.

4. Discussion

4.1. Evaluation of Influence of Slag Thickness on Sensible Heat Recovery by Heat Transfer Analysis

To achieve a high heat recovery ratio in this development, a slag sensible heat recovery process for heat exchange from slag to air by the countercurrent flow packed bed method was assumed. A heat transfer calculation was performed with a 1-dimensional countercurrent flow packed bed heat transfer analysis model, and the appropriate slag thickness for slag sensible heat recovery was examined.

The outline of the heat transfer analysis model is shown in **Fig. 19**. The calculation conditions are shown in **Table 4**. The production rate is 60 t/h, the diameter of the heat recovery tank is 3 m, the height of the slag bed is 3 m, and the filling fraction is 0.41. The shape of the slag was assumed to be a flat plate with dimensions of 50 mm×20 mm, and calculations were made at thicknesses of 3–20 mm. The thermal conductivity is based on Fig. 16. The average specific heat capacity of Cp=1.01 J/(g·K) from 969 K to 1 574 K in Fig. 17 is used.

The slag thickness is assumed to be 2x, and the temperature distribution in the slag is calculated by Eq. (1).

$$\rho C_p \frac{\partial T}{\partial t} = \frac{\partial}{\partial x}\left(\lambda \frac{\partial T}{\partial x}\right) \quad \text{..... (1)}$$

Where, ρ is density [kg/m^3], C_p is specific heat [J/(kg·K)], λ is thermal conductivity [W/(m·K)], T is temperature [K] in the slag, and t is time [s].

The heat transfer coefficient is calculated by Jhonson-Rubesin's equation[25] for the turbulent heat transfer of a flat plate.

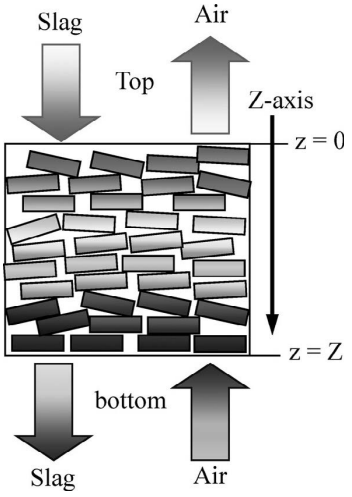

Fig. 19. Calculation method of heat transfer for heat exchange between slag and air.

Table 4. Conditions of heat transfer calculation for heat recovery plant.

Heat transfer system	Countercurrent flow
Size of heat recovery chamber	Φ3 m×H3 m
Heat loss from chamber wall	10 kW/m^2
Feed rate of hot slag	60 t/h
Residence time	20 min
Filling fraction	0.41
Temperature of input slag	1 373 K
Shape of slag	W50 mm×L20 mm
Thickness of slag	3, 4, 5, 7, 10, 15, 20 mm
Air flow rate for heat exchange	50 000 m^3/h
Temperature of input air	298 K

$$Nu = 0.037\,\mathrm{Re}^{4/5}\,\mathrm{Pr}^{1/3} \quad \text{..... (2)}$$

Figure 20 shows the slag and gas temperature distribution in the heat recovery chamber by heat transfer calculation. When the thickness is 7 mm, the difference between the surface temperature and average temperature of the slag is small, and the air temperature at the top of the packed bed is 1 090 K. However, when the thickness is 15 mm, the difference between the surface temperature and average temperature of the slag is large, and the air temperature at the top of the packed bed decreases to 934 K. Because the thermal conductivity of slag is low, the temperature gradient between the surface and center increases as the slag thickness increases. This means that thicker slag is disadvantageous for heat recovery.

Figure 21 shows the effect of the slag thickness on the heat recovery ratio and recovery gas temperature by heat transfer calculation. The heat recovery ratio and recovery gas temperature increase as the slag thickness decreases. As the slag thickness increases, unrecovered sensible heat increase due to discharge of high temperature slag from the bottom of the packed bed. The heat recovery ratio is calculated at 40% at a slag thickness of 7 mm, which was obtained at a roll rotational speed of 7–10 rpm in the twin

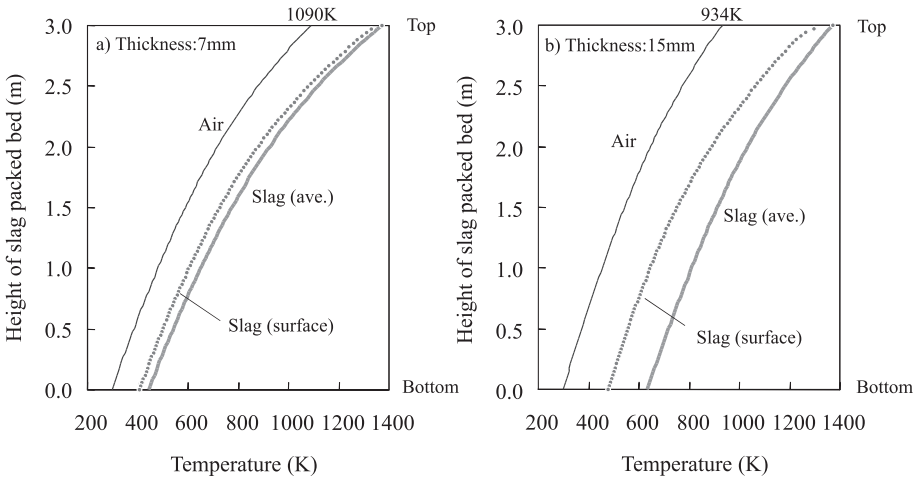

Fig. 20. Slag and gas temperature distribution in heat recovery chamber by heat transfer calculation.

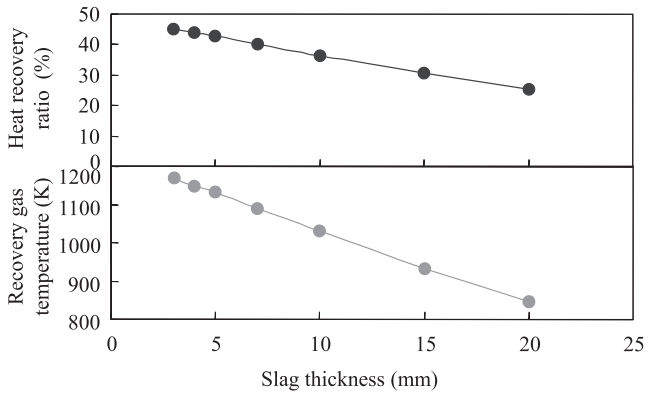

Fig. 21. Effect of slag thickness on heat recovery ratio and recovery gas temperature by heat transfer calculation.

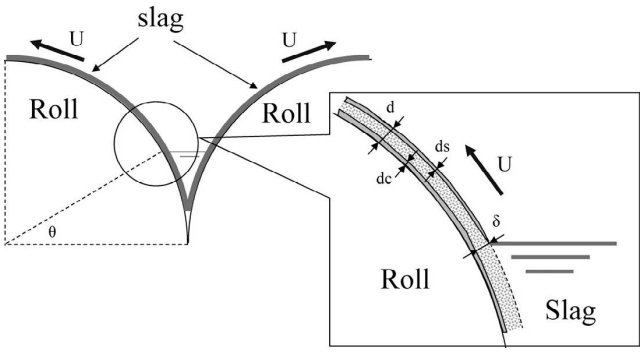

Fig. 22. Schematic diagram of slag shaping on cooling rolls.

roll pilot experiment. 45% of sensible heat is lost in the cooling period on the rolls and conveyor. Reducing the slag thickness is effective for efficient recovery of the remaining 55%.

4.3. Thickness of Sheet-shaped Slag

The thickness of the sheet-shaped slag formed by rolls, and the difference between the twin roll pilot experiment and the single roll laboratory experiment are discussed in the following. In the result of the twin roll pilot experiment in Fig. 13, the solidification thickness was 7–8 mm at the roll rotational speed of 10 rpm. The solidification thickness in the twin roll pilot experiment was about twice that in the single roll laboratory experiment. From observation of the two experiments, slag seemed to adhere on the rotating rolls in the semi-molten state. In this case, the situation of roll forming is estimated to be as shown schematically in **Fig. 22**. Namely, the roll contact face is cooled and solidified. High viscosity molten slag adheres on the solidified slag, and is rolled up with the rotating rolls. It is assumed that the slag is cooled from the roll contact face and the surface after being rolled up.

First, the solidification thickness on the roll contact face will be discussed. The influence of the rotational speed on the slag solidification thickness in the twin roll pilot experiment was calculated by 1-dimensional unsteady heat transfer analysis. The slag is cooled while in contact with the roll surface for one half-turn of the roll. The depth of the slag bath between the rolls is assumed to be from the contact point of the two rolls to rotation by 30°. The thickness of the slag on the roll is assumed to be 7 mm. It is assumed that only cooling from the roll occurs in the slag bath, and additional cooling from the slag surface by thermal transport and radiation occur outside the slag bath. It is assumed that the initial temperature of the slag bath is 1 673 K and the slag solidifies at 1 400 K or less. The thermal conductivity used here is the value in Fig. 16. The specific heat is the value in Fig. 17, *i.e.*, Cp=4.42 J/(g·K) between 1 574 K and 1 723 K.

Figure 23 shows the results of calculation of the slag solidification thickness on the roll contact face. In this figure, 30° means in the slag bath between the rolls and 180° means a half-turn of the roll. The solidification thickness decreases with increasing rotational speed. However, the calculated result is smaller than the observed thickness. The calculated thickness at 10 rpm is estimated to be about 0.5 mm at 30° and about 1 mm at 180°. This calculation indicates that only the vicinity of the roll contact face is quenched.

Figure 24 shows an image analysis of the slag cross section by EPMA. Here, the upper line shows the measured results for the surface (vicinity of atmosphere), the middle line shows the results for the center, and the lower line shows the vicinity of the roll contact face. Because the slag supplied to the roll is not a 100% liquid phase, a primary crystal MgO phase can be seen at all positions. Ca, Si, and

Al are distributed almost uniformly at the roll contact face, excluding the area of precipitation of the crystals of $2CaO{\cdot}SiO_2$ approximately 10 μm in size.

On the other hand, the $2CaO{\cdot}SiO_2$ phase and $2CaO{\cdot}Al_2O_3{\cdot}SiO_2$ phase divide clearly in the order of surface (atmosphere) and center. Cross-sectional observation confirmed that the cooling rate of the slag increases from the center to the surface and the roll contact face in that order. In particular, the small crystal grains indicate that the roll contact face was quenched.

In molten zinc plating, it is well known that the adhesion thickness increases as the speed of the sheet or the roll increases.[26] Moreover, Ueda *et al.*, who studied a technique for recovery of oil from the sea surface by a rotating plate, derived the thickness of a liquid adhering to a vertically-rising plate from Navie-Stokes's equation as follows.[27] Where, δ is liquid thickness [m], μ is viscosity [Pa·s], ρ is density [kg/m^3], g is acceleration of gravity [m/s^2], and U is upward velocity of the plate [m/s].

$$\delta = \sqrt{\mu U / \rho g} \quad \text{..... (3)}$$

Because the rolls are rotated, the steady point of adhesion thickness is uncertain. It is assumed that the adhesion thickness steadies at the top of the slag bath. From the roll rotational speed U[m/s] and the top surface angle of the slag bath θ, the slag adhesion thickness δ is shown by the following Eq. (4).

$$\delta = \sqrt{\mu U / \rho g \cos\theta} \quad \text{..... (4)}$$

The adhesion thickness is estimated by Eq. (4). Here, the viscosity of the molten slag is based on Fig. 18, and is determined at the temperatures of the single roll laboratory experiment and twin roll pilot experiment. **Figure 25** shows the relationship between the experimental slag thickness and calculated slag thickness, which is the sum of the adhesion thickness δ and solidification thickness dc. The thickness of sheet-shaped slag is considered to be determined by the adhesion thickness of the molten slag on the rolls. If the

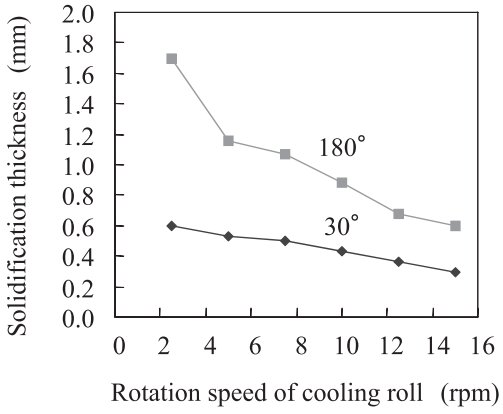

Fig. 23. Calculation results of slag solidification thickness on cooling rolls.

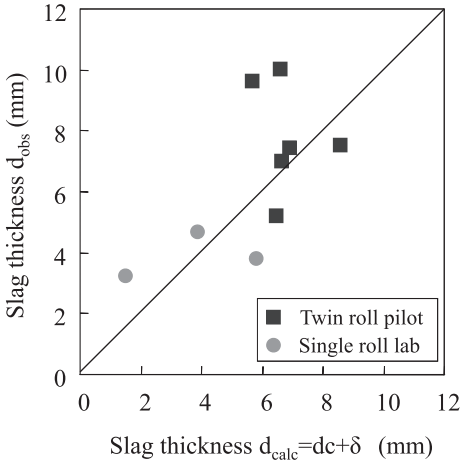

Fig. 25. Comparison of measured and calculated slag thickness.

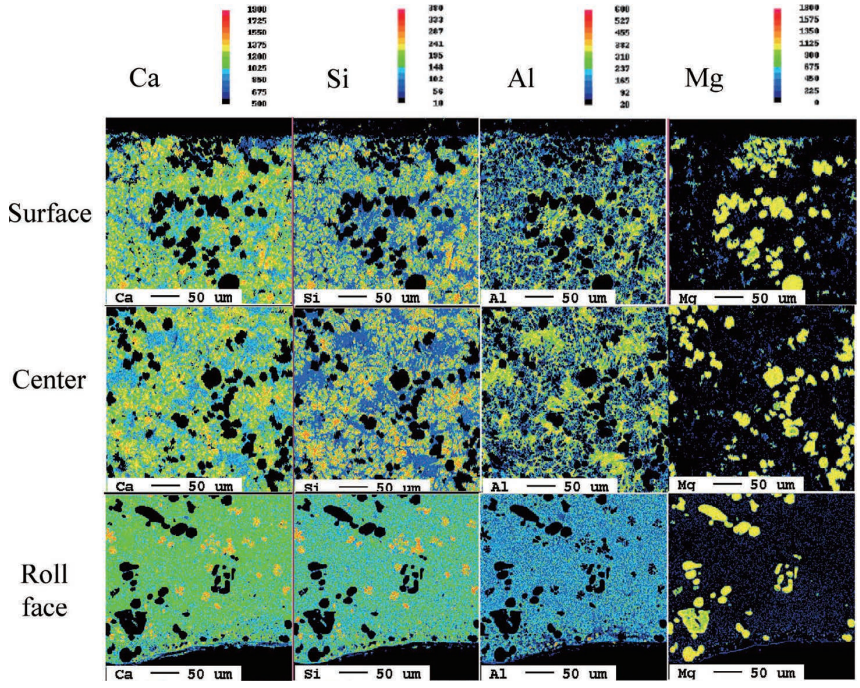

Fig. 24. Image analysis of slag cross section by EPMA.

rotational speeds are the same in the single roll laboratory experiment and twin roll pilot experiment, the contact time of the roll and the slag are also the same, and there is no difference in the solidification thicknesses in contact with the roll face. However, the adhesion thickness in the single roll laboratory experiment is actually greatly different from that in the twin roll pilot experiment. Because the roll diameter of the twin roll pilot plant is Φ1.6 m and that of the single roll laboratory equipment is Φ0.35 m, the circumferential velocity of the former is 4.6 times that of the latter. Furthermore, the slag temperatures were 1 673–1 773 K in the twin roll pilot experiment and 1 873–1 973 K in the single roll laboratory experiment. Therefore, the viscosity of the former slag is about three times that of the latter. Thus, the differences in the circumferential velocity of the rolls and the viscosity of the slag in the single roll laboratory experiment and twin roll pilot experiment appear in the difference in the slag adherence thickness in the two experiments. In Fig. 25, there are cases where the difference between the calculated and observed thicknesses is large. This is considered to be caused by changes in viscosity resulting from temperature changes associated with the residence time between rolls and the slag flow rate, together with fluctuations in the surface level of the slag bath between the rolls.

5. Conclusions

For efficient recovery of the sensible heat of steelmaking slag, which is characterized by low thermal conductivity, a continuous solidification process in which slag is formed to a thin sheet shape by a twin roll method was developed. The following conclusions were derived from the results and discussion.

(1) Steelmaking slag with basicity 2 or more can be solidified continuously by the twin roll method. With a large roll diameter of 1.6 m, the slag adheres to the roll and solidifies in the desired sheet shape.

(2) After cooling by water-cooled copper rolls, the sheet-shaped slag had a high temperature of approximately 1 373 K.

(3) When using a countercurrent flow packed bed for heat exchange from slag to air, a heat transfer analysis showed that the heat recovery ratio and recovery gas temperature increase as the slag thickness decreases.

(4) The fluidity of the slag is important; a liquid phase ratio of 60% or more is suitable for continuously forming sheet-shaped slag by the twin roll method.

(5) The adhesion thickness of molten slag picked up on the rolls is larger than the solidification thickness of the slag after cooling by contact with the rolls. The adhesion thickness is greatly influenced by the circumferential velocity of the rolls and the viscosity of the slag.

Acknowledgment

These results were obtained as part of the project "Environmentally Harmonized Steelmaking Process Technology Development (COURSE50)", which was commissioned by Japan's incorporated administrative agency, the New Energy and Industrial Technology Development Organization (NEDO).

REFERENCES

1) T. Miwa and H. Okuda: *J. Jpn. Inst. Energy*, **89** (2010), 28.
2) S. Tonomura: *Energy Procedia*, **37** (2013), 7160.
3) S. Matsuzaki, K. Higuchi, A. Shinotake and K. Saito: SCANMET IV, Vol. 2, MEFOS, Luleo, (2012), 45.
4) M. Hayashi and T. Mimura: *Energy Procedia*, **37** (2013), 7134.
5) H. Saima, Y. Mogi and T. Haraoka: *Energy Procedia*, **37** (2013), 7152.
6) F. A. Chowdhury, H. Yamada, T. Higashi, Y. Matsuzaki and S. Kazama: *Energy Procedia*, **37** (2013), 265.
7) E. A. Alvarez, A. J. G. Trashorras, J. M. S. Cuesta and J. X. Berrat: *Clean Technol. Environ. Policy*, **14** (2012), 869.
8) M. Sakakibara: *Tetsu-to-Hagané*, **76** (1990), 1587.
9) Y. Kojima, H. Matsui and T. Chikakiyo: *Seitetsu Kenkyu*, (1980), No. 301, 13415.
10) T. Kagawa, M. Tanabe, T. Iwahashi, K. Fujii, T. Shigematsu and T. Nakamura: *Sumitomo Met.*, **34** (1982), 520.
11) H. Fujii: *Kawasaki Tech. Rev.*, **76** (1980), 115.
12) S. J. Pickling, N. Hay, F. Roylance and G. H. Thomas: *Ironmaking Steelmaking*, **12** (1985), 14.
13) T. Nortega, D. Xie and D. Jahanshahi: AISTech Proc., AIST, Warrendale, PA, (2012), 35.
14) H. Purwanto, T. Mizuochi, H. Tobo, M. Takagi and T. Akiyama: *Mater. Trans.*, **45** (2004), 3286.
15) T. Shimizu, G. Mikami, K. Horinouchi and T. Takahashi: *Jpn. Inst. Energy*, **47** (2010), 98.
16) J. Ando, T. Nakahara, S. Tajiri, S. Ichimura, F. Ijima and M. Kondo: *Tech. Rev. Mitsubishi Heavy Industries*, **17** (1980), 915.
17) J. Ando, T. Nakahara, H. Onoue, S. Ichimura and M. Kondo: *Tech. Rev. Mitsubishi Heavy Industries*, **21** (1985), 800.
18) S. Kajikawa, Y. Takahashi, K. Kanai, H. Ito, S. Shinoda and K. Ohgoshi: *Tetsu-to-Hagané*, **68**, (1982), S755.
19) A. Ohta, H. Sato, Y. Sato, H. Ito and Y. Yanagida: *Tetsu-to-Hagané*, **69**, (1983), S844.
20) T. Akashi, S. Doi, T. Kikuchi, N. Suzuki, M. Saruta and T. Teramoto: Symp. on Environmental Engineering, No. 06-10, JSME, Tokyo, (2006), 214.
21) R. Roberti, F. Uberto, M. Svanera, G. Altenburger and F. Cabra: 5th Global Slag Conf, Pro Global Media Ltd., Epsom, (2009), 10.
22) M. Gelti, G. Cornacchia, R. Roberti, M. Svanera and F. Uberto: 7th Global Slag Conf, Pro Global Media Ltd., Epsom, (2011), 10.
23) Y. Kang and K. Morita: *ISIJ Int.*, **46** (2006), 420.
24) A. Seki, Y. Aso, M. Okubo, F. Sudo and K. Ishizaka: *Kawasaki Steel Giho*, **18** (1986), 20.
25) H. A. Johnson and M. W. Rubesin: *Trans. ASME*, **71** (1949), No. 5, 447.
26) T. Fujiwara, T. Kanamaru and M. Nakayama: *Hyomen Gijutsu*, **46** (1995), 1060.
27) K. Ueda, S. Tokuda and N. Isshiki: *J.M.E.S.J.*, **10** (1975), 748.